Publication date: 2021, january 14th

The book,
"PEROVSKITES AND OTHER FRAMEWORK STRUCTURE MATERIALS
(2D-perovskites, Aurivillius, Ruddlesden-Popper, Dion-Jacobson phases, tungsten bronzes, clays, and others)

New trends and perspectives"

(editors P. Saint-Grégoire and M.B Smirnov)

Is a collective volume of 800 pages with **76 authors** and **26 chapters** on recent developments and hot subjects, divided into two parts:

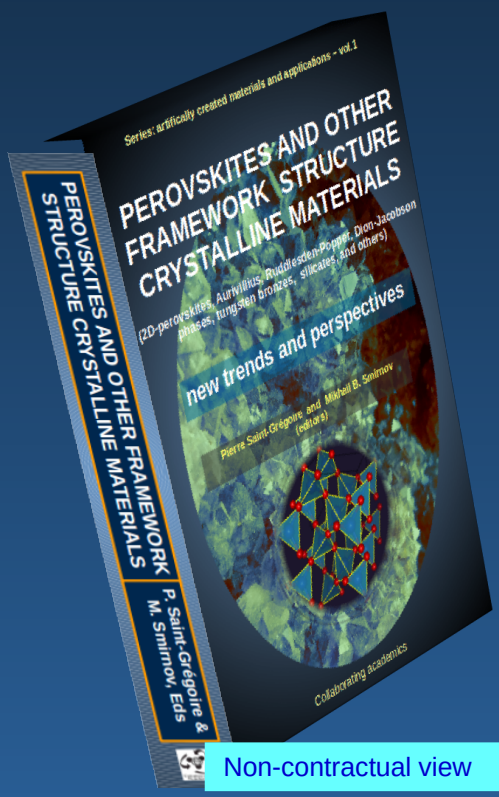

Non-contractual view

A. Fundamental aspects and general properties

B. Elaborated materials and applied properties

Available in 3 formats:

- **Ebook**
- **printed softcover, black & white**
- **printed hardcover, color.**

Go to the Book(click)

Chapter 10 : Trigonal double molybdates and tungstates
Ferroelastic phase transitions

M.B.Zapart and W.Zapart

Institute of Physics, Technical University of Częstochowa, Poland

Corresponding author: zapart@wip.pcz.pl; bozena.zapart@gmail.com

Abstract : The overview contains basic information about trigonal double molybdates and tungstates $MR(XO_4)_2$, representing a crystal family with layered structure. Their structure features networks of corner-linked RO_6 octahedra and XO_4 tetrahedra. Many compounds of this crystal family exhibit ferroelastic phase transitions. Their ferroelastic properties are discussed, with particular emphasis on the peculiarities of the domain structure. An overview of results of studies on ferroelastic phase transitions, obtained with various experimental methods, is provided. Models of trigonal unit cell distortion are presented for monoclinic phases of $KSc(MoO_4)_2$ and $RbIn(MoO_4)_2$ crystals.

Keywords : TRIGONAL DOUBLE MOLYBDATES /TUNGSTATES,LAYERED STRUCTURE, FERROELASTICS, PHASE TRANSITIONS, DOMAIN PATTERNS

Cite this paper: M.B.Zapart and W.Zapart, OAJ materials and Devices, vol 5(1) – chap No10 in "Perovskites and other Framework Structure Crystalline Materials", p327 (Coll. Acad. 2021) DOI:10.23647/ca.md20202708

I. Introduction

Within the last few decades, molybdates and tungstates have been an attractive field in solid-state chemistry and condensed matter physics [1-4]. In particular, double molybdates and tungstates of alkali and trivalent cations with the composition $MR[(Mo,W)O_4]_2$ (where M represents an alkali metal, R - trivalent element (rare-earth, Bi, In, Sc, Ga, Al, Fe or Cr), X stands for W or Mo) include a number of materials with interesting structural and physico-chemical properties. These compounds form a wide crystal family in which different structural types and numerous polymorphic phase transformations have been distinguished [5].

The succession of structural types with change in the ionic radii of R^{3+} and M^{+}, met in double molybdates and tungstates, has been described in a review paper of Klevtsov and Klevtsova [5].The compounds can be listed in 22 structural types distributed into four basic classes taken as parent types: scheelite $CaWO_4$, wolframite $(Fe,Mn)WO_4$, γ-$RbPr(MoO_4)_2$ and glaserite-type (trigonal) $KAl(MoO_4)_2$. Recently the incommensurately modulated scheelite-like structure have been found in $KNd(MoO_4)_2$ [6], $KSm(MoO_4)_2$ [7] and $KEu(MoO_4)_2$ [8].

During last decades the interest to the scheelite and scheelite-like $MR[(Mo,W)O_4]_2$ has been maintained in relation with their several potential applications in solid state laser technology. In particular, these materials doped by rare earth or transition metal ions are attractive laser host materials, promising red and multicolor tunable phosphors for solid-state lighting efficient self-converting Raman crystals [9-17]. A review of the recent advances in the field of bulk lasers based on double tungstates $KY(WO_4)_2$, $KGd(WO_4)_2$, $KLu(WO_4)_2$ and work toward the demonstration of waveguide lasers and their integration with other optical structures on a chip is done in paper [18] .

In this paper we will review the results of studies on trigonal double molybdates and tungstates (briefly TDM/T), with emphasis on ferroelastic phase transitions. TDM/T crystals form a layered subclass of $MR(XO_4)_2$ (where M = K, Rb, Cs and R = Sc, In, Fe, Al, Cr) molybdates and tungstates assigned to the $KAl(MoO_4)_2$ (space group P-3m1) structural type. According to [5], the $NaFe(MoO_4)_2$ (space group C2/c) structural type can also be combined to the $KAl(MoO_4)_2$ one, forming the trigonal double molybdates and tungstates crystal family. The isostructural compounds $NaFe(MoO_4)_2$, $NaAl(MoO_4)_2$ and $NaCr(MoO_4)_2$ in the whole interval up to their melting points possess the ferroelastic properties and may be characterized by the hypothetical para-phase P-3m1 [19-21]. TDM/T show a rich polymorphism; e.g $KIn(WO_4)_2$, $RbIn(WO_4)_2$, $RbIn(MoO_4)_2$ and $CsIn(MoO_4)_2$ may crystallize in two polymorphic modifications, depending on the crystallization metod [5]. At ambient temperature, their high-temperature trigonal (α- form, P-3m1) and the low-temperature orthorhombic (β- form, Pnam)

phases can be obtained. The trigonal variant may be produced by rapid quenching of its high-temperature phase, while a slow cooling gives the β- form.

The trigonal crystal structure of $MR(XO_4)_2$ can be described as networks of RO_6 octahedra sharing vertices with XO_4 tetrahedra [22]. The XO_4 units have two non-equivalent oxygen atoms, namely, O1 and O2 for the oxygen atoms relying closest to M^+ and R^{3+} cations, respectively. Together these polyhedra form layers arranged perpendicularly to the *c* axis (Figure 1a). The infinite two-dimensional sheets $\{[R(XO_4)_2]^-\}_{\infty\infty}$ are separated by layers of M^+ ions which are surrounded by twelve oxygen atoms. Inside the layers, the ions form regular triangular lattices (Figure 1b). The layered $NaFe(MoO_4)_2$-type structure can be regarded as derived from the former structural type by slight rotations of the MoO_4 tetrahedral units and shifts of the Na^+ ions. As in the case of $KAl(MoO_4)_2$, each kind of cation lies in a separate plane perpendicular to the *c* axis [23] .

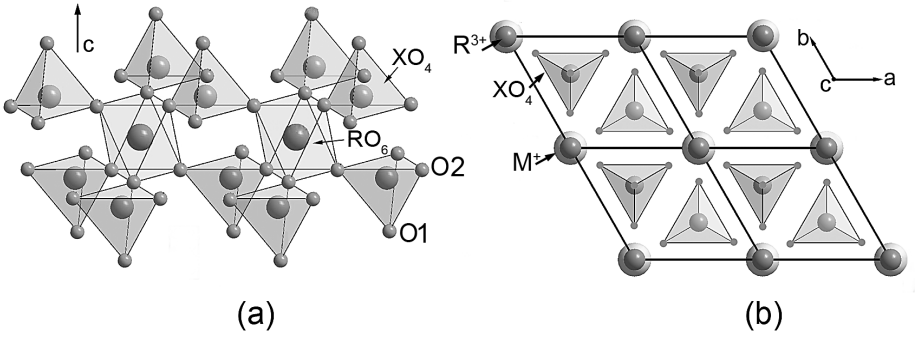

Figure 1: The structure of TDM/T. (a) $[R(XO_4)_2]^-$ polyhedra sheet parallel to the (0001) crystal plane; (b) View of the crystal structure along the c-axis. Pictures are drawn using Diamond program [24].

The basic growth form of the crystals of both structural types shows pseudo-hexagonal character.The crystals crystallize in the form of hexagonal platelets with the most fully developed faces (0001) parallel to the layers and exhibit perfect cleavage.

The most commonly used method of growing TDM/T crystals is the thermal method developed by Klevtsov et al.[25] . However, to obtain bulk crystals of large size and high quality the top seed solution growth (TSSG) technique is applied [26].Nanocrystalline

TDM/T are obtained via the Pechini [27] as well as by co-precipitation/calcination methods [28] .

TDM/T have attracted much attention in recent years because of their simple structure, the ability to undergo ferroelastic phase transitions and critical phenomena which are observed at the variation of temperature, pressure and mixed crystal composition. A phenomenological approach to ferroelastic transitions in TDM/T family [29] relies on the assumption that the transition from the trigonal phase is induced by one of the two-dimensional irreducible representations (τ_5 or τ_6) of the space group P-3m1 and occur between phases : P-3m1 → (C2/m or C2/c) → P-1.

The ferroelastic phase transitions in TDM/T are described by a two-component order parameter **c**[c_1, c_2]. If components of this parameter satisfy condition $c_1 \neq 0$ and $c_2=0$, then a monoclinic system of C2/c symmetry is realised in the crystal, if $c_2 \neq 0$ and $c_1=0$, then a monoclinic system of C2/m symmetry. When both components are different from zero the ferroelastic phase belongs to a triclinic system of P-1 symmetry [29]. A transition from the trigonal to monoclinic phases (C2/m or C2/c) is improper and is accompanied by a doubling of the unit cell along the threefold axis of the crystal. A transition to the triclinic phase P-1 can be a result of the equitranslational transitions from any monoclinic phases, attended by twofold point symmetry reduction [29] .

The ferroelastic transitions occuring in TDM/T are of displacive type and are connected with rotations of the XO_4 tetrahedra and shifts of alkali atoms [30] . The simplest phase transition model which accounts for the unit cell distortions in alternative monoclinic phases C2/m and C2/c corresponds to rotations of rigid tetrahedra around the X axis or Y axis (in the coordinate system XYZ, where X || 2, Z || -3, Y lying in the *m* plane), respectively. Simultaneously, M^+ ions are shifted from their positions at P-3m1 sites along the Y axis in C2/m phase and along the X axis in C2/c phase. The displacements of cations and polyhedra rotations in adjacent layers of the structure are in antiphase, the result being the unit cell doubling along the crystal threefold axis. In the C2/c phase all ions are crystallographically equivalent, whereas in the C2/m structure both trivalent ions and XO_4 tetrahedra occupy two non-equivalent sites.

Ferroelastic phase transitions are accompanied by onset of spontaneous strain and nucleation of ferroelastic domains. The trigonal-to-monoclinic symmetry reduction results in appearance of the spontaneous strains e_1 - e_2 and e_4 [29]. The ferroelastic domains in the monoclinic phases can be switched by stresses $\sigma_1 - \sigma_2$ and σ_4 .The formation of ferroelastic domain structure, and geometrically permissible domains packings in the TDM/T crystals in their monoclinic phases were studied under a microscope in the polarized ligth [19,31-36]. The process of ferroelastic domains switching in monoclinic phases is described in [37-39]. Studies of domain structures in TDM/T with domain sizes below 1 μm were carried out by methods of electron transmission (TEM) [40] and atomic force (AFM) [41,42] microscopy.

Table 1: Crystallographic data and temperatures of structural phase transitions for P-3m1 structure

Compound	Space group	Unit cell parameters [nm]	Phase transition temperatures and experiment
$KAl(MoO_4)_2$	P-3m1 Z=1 a, c γ=120º	0.5545 0.7070 [22]	T_1=90 K [43] Raman & IR T_2=50 K [44] EPR
$KFe(MoO_4)_2$		0.5672 0.7114 [45]	T_1=311 K [46] PLM T_2=139 K [47] HC
$KSc(MoO_4)_2$		0.5772 0.7207 [22]	T_1=260 K [29] PLM T_2=240 K [48] EPR T_3≈183 K [29] PLM
$KSc(WO_4)_2$		0.5791 0.7186 [49]	T_1=307 K [46] PLM T_2=288 K [50] EPR T_3=124 K [51] EPR
α- $KIn(WO_4)_2$		0.580 0.725 [52]	T_1=499 K [53] PLM $T_{\alpha\rightarrow\beta}$=1123 K [54] DTA
α - $RbIn(MoO_4)_2$		0.5817 0.7523 [55]	T_1=163 K [56] EPR T_2=143 K [57] PLM; EPR T_3=134 K [58] EPR T_4= 98 K [59] EPR; PLM T_5= 84 K [60] EPR;PLM;DMA $T_{\alpha\rightarrow\beta}$=1058 K [54] DTA
$RbSc(MoO_4)_2$		0.5793 0.7568 [49]	No phase transition [29,46] PLM
$RbFe(MoO_4)_2$		0.5689 0.748 [22]	T_1=190 K [61] X-ray diffraction
$RbAl(MoO_4)_2$		0.5545 0.7470 [45]	No phase transition [62] Raman & IR
$RbSc(WO_4)_2$		0.581 0.756 [54]	No phase transition [29,46] PLM
α-$RbIn(WO_4)_2$		0.583 0.759 [54]	T_1=90 K [46] PLM $T_{\alpha\rightarrow\beta}$=1088 K [54] DTA
$CsFe(MoO_4)_2$		0.5609 0.8051 [45]	T_1=220 K [63] Neutron diffraction
$CsAl(MoO_4)_2$		0.5551 0.8037 [64]	No phase transition [64] X-ray diffraction
$CsSc(MoO_4)_2$		0.5809 0.8051 [49]	T_1=16 K [65] EP

Raman & IR – Raman and infrared spectroscopy
EPR – electron paramagnetic resonance spectroscopy
PLM- polarized ligth microscopy
HC- heat capacity measurement
DMA – dynamic mechanical analysis
DTA – differential thermal analysis
EP – electric permittivity

According to the phenomenological approach the twofold point symmetry reduction accompaning the transitions (C2/c, C2/m)→ P-1 corresponds to strains (spontaneous deformations) e_5 and e_6 and the ferroelastic domains in the triclinic phase can be switched by applying stresses σ_5 , σ_6 [29] .

Structure data and temperatures of structural phase transitions (including polymorphic transitions α→β) in the TDM/T family are presented in Table 1 and 2. In addition, experimental methods used to determine the phase transitions temperature are quoted.

Usually, one or two ferroelastic phase transitions take place in the TDM/T crystals. For example, $KIn(WO_4)_2$[34] undergoes one phase transition, but two ferroelastic transformations take place in $KAl(MoO_4)_2$ [43,44] and $KFe(MoO_4)_2$ [46,47]. Sometimes, like in the case of $KSc(MoO_4)_2$ [29,48] and $KSc(WO_4)_2$ [46,50] there occur three ferroelastic transitions. In this family, $RbIn(MoO_4)_2$ seems to show the richest variety of structural phase transitions (the points from T_1 to T_5), with three different ferroelastic phases [56-60]. In some TDM/T crystals no phase transition occurs (Table 1). Structural phase transitions occuring at T_1 in $RbFe(MoO_4)_2$ [61] and $CsFe(MoO_4)_2$ [63] lead to non-ferroelastic phases (P-3 system).

Table 2: Crystallographic data and temperatures of structural phase transitions for C2/c structure

Compound	Space group	Unit cell parameters [nm]	Phase transition temperature and experiment
$NaFe(MoO_4)_2$	C2/c Z=4 a,b,c β	0.987; 0.531; 1.357 90.4° [24]	T_{melt} =973 K $T_1 > T_{melt}$ [19] PLM
$NaAl(MoO_4)_2$		0.9621;0.5339;1.3146 90.01° [66]	T_{melt} =913 K [31] T_1 ≈813 K; T_2= 703 K [31] PLM $T_1 > T_{melt}$ [67] Raman T_1 = 780 K [21] DTA
$NaSc(MoO_4)_2$		No structure data	T_1=763 K; T_2=333 K [20] PLM
$NaAl(WO_4)_2$		0.963; 0.5373; 1.2978 90.2° [68]	T_{melt} =973 K $T_1 > T_{melt}$ [69] Raman

Inconsistent data as to a phase transition temperature in $KIn(WO_4)_2$ are reported in literature. In the early 80's, from microscopic studies it has been shown [34] that the structural transition from a trigonal to monoclinic system in $KIn(WO_4)_2$, resulting in a ferroelastic ordering, occurs at T_1=454 K. Much later, based on infrared and Raman spectroscopy [70] a higher transition temperature was obtained. Its value (475 ±16 K) was found from the fitting the data of the split Raman-active band as the function of temperature. Recently, our microscopic observations [53] of $KIn(WO_4)_2$ reveal a poor colour differentiation of the sample and the appearance of ferroelastic domain structure at T_1 = 499 K. The fact that the transition seen in the Raman experiment appears at lower temperature (475 K) may be explained by a laser heating which induces temperature differences between the sample and thermocouple attached to the metal sample holder [77].Contradictory results are also reported on phase transitions in $NaAl(MoO_4)_2$. In the 70's it was reported [31] that this material had two phase transitions, one close to 703 K (430°C), and the second one above 813 K (640°C), which was said to be the transition to the trigonal phase. Based on Raman studies [67] it was found that $NaAl(MoO_4)_2$ remains in the monoclinic structure up to the melting temperature. Neither soft modes were detected nor changes in the Raman spectrum were observed which would refer to the transition at 703 K. Little later, from differential thermal analysis, a reversible phase transition from the monoclinic to the trigonal phase in $NaAl(MoO_4)_2$ was reported at 780 K [21].

Investigations of dielectric properties of TDM/T with M=K, Rb have shown that they possess a low dielectric constant (≈ 5) weakly dependent on temperature [29, 71, 72]. Phase transitions from the trigonal phase are accompanied by very weak anomalies, namely by a kink of the $\varepsilon_c(T)$ curve. In the low-symmetry phase ε_c gradually rises with cooling and reaches values about 0.5% higher than $\varepsilon_c(T_1)$.

The ferroelastic transitions in TDM/T have been evidenced by anomalies in the Raman [30,47,67,70,73-79] and Brillouin spectra [74,75,80,81], ultrasonic studies [82], x-ray measurements [83-85], heat capacity [86] as well as in electron paramagnetic resonance (EPR) spectra [48,50,51,53,56-60,83,87-97]. Re-building of the ferroelastic domain structure in compounds exhibiting a sequence of phase transitions has been observed using a polarized-ligth microscopy [60,95,96,98-103].

In spite of the fact that crystals have attracted the attention of researchers for a number of years, there still seem to be a lot of doubts regarding their properties. In some crystals belonging to this family, such as $KSc(MoO_4)_2$, $RbIn(MoO_4)_2$, and $KSc(WO_4)_2$, transitions to simultaneously incommensurate and ferroelastic phases have been suggested [48,83,104-109]. Thus, the crystals may be said to be examples of systems described by a multi-component order parameter. A brief overview of incommensurately modulated improper ferroelastics is given in [110].

In the layered TDM/T compounds, the temperature of trigonal-monoclinic phase transition (T_1) depends strongly on the interlayer interactions and it decreases with increasing size of alkali metal ion [29] (see Table 1). For instance, in the case of scandium compounds the transition temperature changes from 16 K for $CsSc(MoO_4)_2$ [65] to 763 K for $NaSc(MoO_4)_2$ [20] . In order to explain the role of alkali metals in the stability of the trigonal phase in TDM/T crystals studies on mixed crystals $(KX)Sc(MoO_4)_2$ (X = Rb, Cs, Na, Li) were carried out [65,111-117] . The effect of reducing the distance between layers (the transition from two- to- three dimensionality of TDM/T crystal lattice) on the value of temperature T_1 was studied in [71,118] .

High-pressure studies of layered TDM/T through Raman spectroscopy were performed for four compounds: $KSc(MoO_4)_2$ [119], $NaAl(MoO_4)_2$ [120], $KFe(MoO_4)_2$ [121] and $RbFe(MoO_4)_2$ [122, 123] . Results of these studies will not be discussed here because a comprehensive overview of pressure induced phase transitions in molybdates and tungstates is provided in [124] .

Quite recently, iron containing molybdates $KFe(MoO_4)_2$ [125,126], $RbFe(MoO_4)_2$ [127-129] and $CsFe(MoO_4)_2$ [63] have attracted a lot of attention since they turned out to be good models of nearly 2-D triangular lattice antiferromagnets. Moreover, $RbFe(MoO_4)_2$ displays a zero-field magnetically driven multiferroic phase with a chiral spin structure [129] . Cr^{3+}-doped TDM/T materials can also be considered as potential candidates for broadband laser applications [26,130] .

In the next section we shall discuss characteristic features of ferroelastic domain patterns in TDM/T crystals.

II. Pecularities of ferroelastic domain structure in TDM/T

Ferroelastic domains appear as a consequence of the reduction in symmetry between the paraelastic and ferroelastic phases. From studies of domain structure (DS) patterns in TDM/T under a polarizing microscope it was stated that the domains formed below T_1 correspond to three orientational states acceptable for ferroelastics of the -3mF2/m species [130]. The domains are separated by two types of permissible planar domain walls, vertical W coinciding with the mirror planes lost at the phase transition and tilted W`, the orientation of which depends on relative value of components of the spontaneous strain (deformation) tensor [131]. For example, the slope of W` walls, i.e. an angle θ between W`and the normal to (0001) planes, is following : in $KIn(WO_4)_2$ θ = 55°18`±10` and in $KFe(MoO_4)_2$ θ = 49°±3° [34] , whereas in $NaFe(MoO_4)_2$ θ = 6°±1° [36]. As the K^+ ion is replaced by Na^+, the angle of inclination of

the domain walls W` in solid solutions $Na_xK_{1-x}Fe(MoO_4)_2$ changes in the range from 5º to 50º [35].

In TDM/T there are no equilibrium DS containing the regular domain packings of all the three orientational states since the formation of such DS is impeded by elastic stresses resulting from the intersection of domain walls planes along mutual edges of the adjacent domains [34] . Geometrically permissible variants of the -3mF2/m ferroelastic partition into three orientational states by W, W` walls, leading to unstable DS, have been discussed in [34].

In TDM/T there is a tendency to form polysynthetic domain structures: twins $T_W(W)$ or $T_W(W`)$ consisting of very thin lamellae, where W and W` planes serve as twin boundaries [32,34,98]. Moreover, the different occurrence of straight and tilted walls in the DS has been found [32,34] . For example, the existence of tilted W` walls and formation of polysynthetic twins Tw(W`) are preferable in $KIn(WO_4)_2$. On the contrary, in $KFe(MoO_4)_2$ the equilibrium DS represents polysynthetic twins Tw(W) with vertical W walls. The characteristic for $KFe(MoO_4)_2$ twinning $T_W(W_i)$ (i=1,2,3) with the periodic domain structure is illustrated in Figure 2.

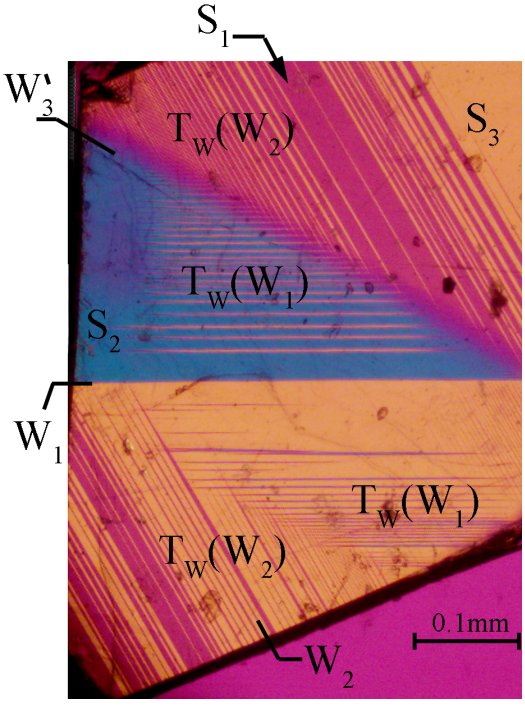

Figure 2: Domain pattern in $KFe(MoO_4)_2$ at room temperature ($T<T_1$) under crossed polarizers.

Some peculiar features of DS are displayed when rival polysynthetic twins with the different orientation of domain boundaries develop in the crystal. The interaction of polysynthetic twins, Tw(W_j) and Tw(W_k) can produce the tilted W`$_i$ wall at their intersection [34] . Such a case is visible in Figure 2 in the area of overlapping the two twin systems Tw($W_1$) and Tw($W_2$); the mutual for both twins domain $S_3$ disappears and the single W`$_3$ wall is formed.

It has been shown that quasiperiodic polysynthetic twins with tilted twin planes W` and with very small periods possess unusual crystallooptical properties [98]. In particular, their extinction positions depend on a relative content of orientational states $S_j$ and $S_k$ (j, k≠ i) in a twin structure Tw(W`$_i$).

The more complicated DS with zig-zag boundaries of two types, Z and Z`, can also be found in the domain patterns of TDM/T [32,34]. The Z and Z` can separate the same domain pairs that simple walls W and W', respectively. In mechanically free crystals, they are unstable and disappear quickly.

TDMs are characterized by the great ease of mechanical re-arrangement of domain structures, which can occur both by moving all types of domain walls and by forming new domains [38]. Ferroelastic hysteresis loops of $KFe(MoO_4)_2$ exposed to uniform and inhomogeneous loads are reported in [37,38]. A small width of the hysteresis loop and a high switching speed is stated for TDM/T. The domain switching was carried out under strict uniaxial loading (σ_1 or σ_2) of the sample along X- (X || 2) or Y- axes. The threshold stress of the onset of domain wall motion in $KFe(MoO_4)_2$ is 0.05 N/cm^2, and the monodomainization is completed at stress of 5 N/cm^2. The full mono-domainization of $NaFe(MoO_4)_2$ is achieved at about 20 N/cm^2 [33]. It was stated that transitions at lower temperatures in $KFe(MoO_4)_2$ and $KSc(MoO_4)_2$ do not affect the hysteresis loop [38]. Furthermore, the domain walls in TDM/T are characterized by very high mobility, e.g. their speed in $KFe(MoO_4)_2$ reaches 4 m/s under a stress of 4 N/cm^2 [38] .

The trigonal-to-monoclinic phase transition is characterized by two components of spontaneous deformation tensor: $a_1 = ½ (e_1 - e_2)$ and e_4. These values, obtained on the basis of knowledge of the unit cell parameters in the trigonal and ferroelastic phase, are as follows: in $KFe(MoO_4)_2$ $a_1 = 2.35x10^{-3}$ and $e_4 = 2.91x10^{-3}$ [35], in $NaFe(MoO_4)_2$ $a_1 = 7x10^{-2}$ and $e_4 = 7x10^{-3}$ [35], and in $KIn(WO_4)_2$ $a_1 = 2x10^{-2}$ [39], $e_4 = 2.91x10^{-3}$ [32]. Because distortions of the trigonal unit cell are opposite in alternative monoclinic phases, phases C2/m and C2/c should differ with the sign of spontaneous deformation a_1 [29]. In ferroelastics with three orientational states (120° domains) [133], the sign of the stress σ_1 (σ_2), which switches the crystal to the only stable state, must coincide with the sign of spontaneous deformation a_1. Thus, the determination of the sign of monodomainizing stress can be used to identify the spatial symmetry of monoclinic phases formed during the considered phase transitions [39] .

The structural phase transitions from the P-3m1 phase are accompanied by changes of the character of optical anisotropy. After the phase transition at T_1 the uniaxial (negative) TDM/T become biaxial (negative). Opposite unit cell distortions in phases C2/m and C2/c result in different disposition of the principal axes of optical indicatrix in the (0001) plane relatively to the internal symmetry elements of domains: the axis n_g is parallel to the two-fold axis (n_g || 2) of the crystal and n_m || *m* in C2/m phase and n_g || *m* and n_m || 2 in C2/c phase [36,99,100].

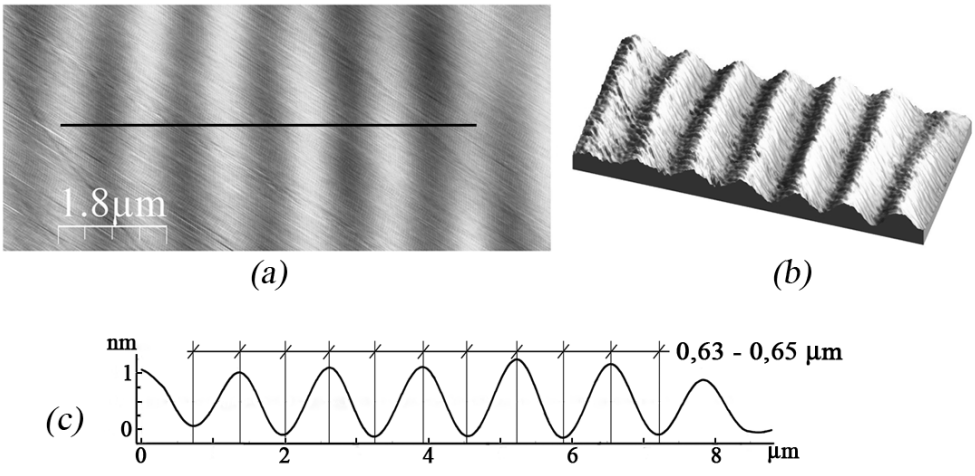

Figure 3: Ferroelastic domain structure observed on the surface of $KSc(WO_4)_2$. (a) AFM image; (b) AFM image in a three-dimensional view; (c) the cross-section along the line marked in (a) [42].

At room temperature the morphology of the freshly cleaved surface (0001) in $KAl(MoO_4)_2$ [134] , $KFe(MoO_4)_2$ [41] , $KSc(WO_4)_2$ [42] and $NaFe(MoO_4)_2$ [42] was examined by atomic force microscopy (AFM). The images revealed stepped surfaces with step heights corresponding to multiples of their crystal lattice constant *c* in the para-phase. Also the surface deformation caused by a presence of ferroelastic domain structure was imaged. The cleavage plane forming a zig-zag profile along domain walls W was observed in $KFe(MoO_4)_2$ [41] . It was found that the crystal surfaces bend at the domain boundaries by the angles which can be explained in terms of the monoclinic distortions [41]. In addition to the regular parallel arrangements of domains, more complex patterns of DS in $KFe(MoO_4)_2$ were visualized, i.e. needles-like structure as well as overlapping domains which have been also observed optically [41].

The topography of the intersection of ferroelastic domains in $KSc(WO_4)_2$ with the (0001) plane is shown in Figure 3.

Ferroelastic domains of very different widths, dependent on the specimen and the measuring point, were observed. In $KFe(MoO_4)_2$, the domain widths were varying from a fraction of μm to a few μm [41]. In $KSc(WO_4)_2$, most domains were characterized by a width of about 0.63 - 0.65 μm (Fig. 3), whereas in $NaFe(MoO_4)_2$ the domain size was of the order 0.9 - 1.0 μm [42].

III. Ferroelastic phase transitions in selected TDM/T

Electron paramagnetic resonance (EPR) spectroscopy is not able to penetrate the crystal structure as deeply as diffraction methods (e.g. X-ray), however, compared to these methods it is two orders of magnitude more sensitive to changes in the coordination environment of ions active in EPR spectroscopy. Therefore, in combination with other research methods, it can become a source of valuable information regarding both the nature of structural phase transitions and the local ordering in the crystal structure of low-temperature phases.

That is why EPR spectroscopy of admixture ions, used in our laboratory, has been turned out so succesful in studying the ferroelastic phase transitions in TDM/T family. Based on literature data on the research, carried out over several decades by various methods, ferroelastic phase transitions in selected members of the TDM/T crystal family are presented in this section.

III.1 $RbIn(MoO_4)_2$

The trigonal form of $RbIn(MoO_4)_2$ seems to exhibit the richest sequence of structural phase transitions in the family of double trigonal molybdates and tungstates. Phase transitions were evidenced by anomalies seen in EPR spectra, and changes in the ferroelastic domain structure as well as through dynamical mechanical analysis (DMA).

EPR of admixture ions led to the detection of a second order phase transition at T_1=163 K [56]. This transition is visible in the EPR spectra both through resonance line amplitude and shape changes; the EPR lines are substantially broadened and unresolved below T_1 [58]. X-ray investigations indicate that in the vicinity of 163 K

anomalies in the temperature dependence of the lattice constants *a* and *c* occur [83]. Also the electric permittivity shows an anomaly in the neighbourhood of 163 K [83].

Most striking was the fact that this phase transition is not accompanied by appearance of ferroelastic domain structure [57]. This structure becomes visible not earlier than around T_2=143 K and the domain configuration observed in different thermal cycles is based on the W and W` walls. Lowering of the crystal symmetry in the vicinity of 143 K was also evidenced in the conoscopic images of $RbIn(MoO_4)_2$ [57]. The appearance of ferroelastic domain structure at 143 K coincides with another anomaly observed in the EPR spectra; the resonance lines increase their amplitude and each of the original lines is split into three broad lines. These experimental findings can be well understood under the assumption that the transition at T_1 = 163 K takes the crystal from a trigonal to incommensurate 3*q* phase, and then to a three-domain 1q state at T_2 = 143 K [83,90,107].

It has been found that the ferroelastic phase transition observed around 143 K is split into two transitions separated by a very small temperature interval of about 0.2 K. These phases coexist in a temperature range of few dozen degrees [95].

On further lowering the temperature anomalies in the EPR spectra point at subsequent transitions at T_3 = 134 K and T_4 = 98 K [58,59]. A stable arrangement of domains formed at T_2 does not undergo significant reconstruction in the region near T_3. The domain structure is completely rebuilt at T_4 = 98 K and, as result, large domains separated by the W walls predominate [57].

The morphic birefringence and changes in the orientation of the optical indicatrix axes n_g and n_m in all the ferroelastic phases occuring in $RbIn(MoO_4)_2$ were studied [101]. The location of optical indicatrix axes in the temperature region 98 - 143 K can be summarized as follows: n_m is parallel to the two fold axis (n_m || 2) and n_g lies in the mirror symmetry plane (n_g || *m*). A change in their orientation takes place at 98 K and we have n_g || *2* and n_m || *m*. Such orientations of principal axes of indicatrix are expected for the monoclinic phases. This means that ferroelastic phase transitions observed in $RbIn(MoO_4)_2$ at T_3 and T_4 should separate different modifications of the monoclinically arranged structure. Two transitions occurring at the temperatures T_2 = 143 K and T_4 = 98 K are visible through abrupt changes in the double refraction, whereas the transition at T_3 = 134 K is marked by only a very slight change of the effect size. Based on the earlier EPR results and optical measurements the monoclinic C2/c symmetry is suggested for the first two ferroelastic phases, and C2/m symmetry for the third phase.

The sequence of phase transitions in $RbIn(MoO_4)_2$ ends up with a transition at T_5 = 84 K, after which the trigonal symmetry seems to be restored [60]. The ferroelastic domain structure disappears below this transition point and the crystal, like at temperatures higher than 143 K, shows no ferroelastic properties. This transition was confirmed by

DMA through anomalies in the temperature behavior of both real and imaginary parts of the Young's modulus [60] .

Below T_5, instead of broad and overlapping EPR lines observable in the EPR spectrum in the temperature range from 85 K to 98 K, seven intense well-separated resonance lines appear (Figure 4). Their emergence cannot be explained within the theory of ferroelastic phase transitions leading from the trigonal phase to lower symmetry phases.

The disposition of the principal axes of Cr^{3+} complexes showing the Laue class -3m, as found from the anisotropy patterns taken at 77 K [60] , and the lack of the ferroelastic domain structure below 84 K indicates that, despite large changes in the crystal structure, the transition to the lowest phase restores the trigonal symmetry.

Thus, admissible point groups of the $RbIn(MoO_4)_2$ in the lowest temperature phase can be -3m, 3m or 32. The first point group coincides with the point symmetry of the high temperature paraelastic phase of $RbIn(MoO_4)_2$. The two latter ones would allow the ferroic species -3mF32(or 3m) [60]. In these three point groups the positions of symmetry – either -3m or 3m or 32 – could be recognized in the unit cell.

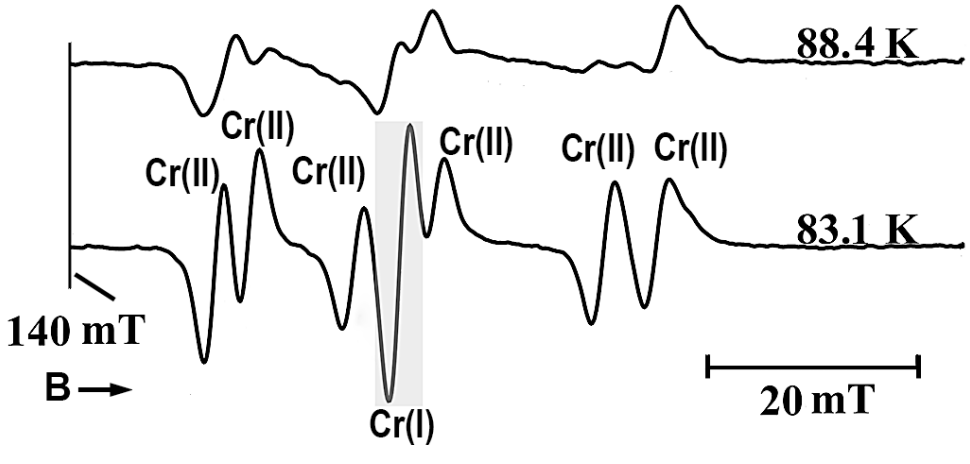

Figure 4: EPR lines of chromium complexes in $RbIn(MoO_4)_2$ in a close vicinity of T_5. EPR transition I1/2>→ I-1/2>, a magnetic field perpendicular to the crystal Z axis.

The Cr^{3+} ions occupying lattice positions of the -3m, 3m or 32 symmetry yield EPR lines which would mimic the EPR lines of the high temperature phase (type I).The Cr^{3+} ions occupying the positions of lower symmetry give six magnetically non-equivalent

centres described by the same spin Hamiltonian parameters but differing in their principal axes disposition (type II).

A scheme of possible distortion of the trigonal unit cell that explains the presence of two groups of Cr^{3+} complexes (I and II) is shown in Figure 5. The arrows indicate changes in the positions of O2 oxygen ions compared to their positions in the high temperature trigonal phase. The signs" plus" and "minus" at the O2 oxygen ions denote the direction, in which their *z*-component varies compared to that in the trigonal phase. The chromium complexes of type I are shaded.

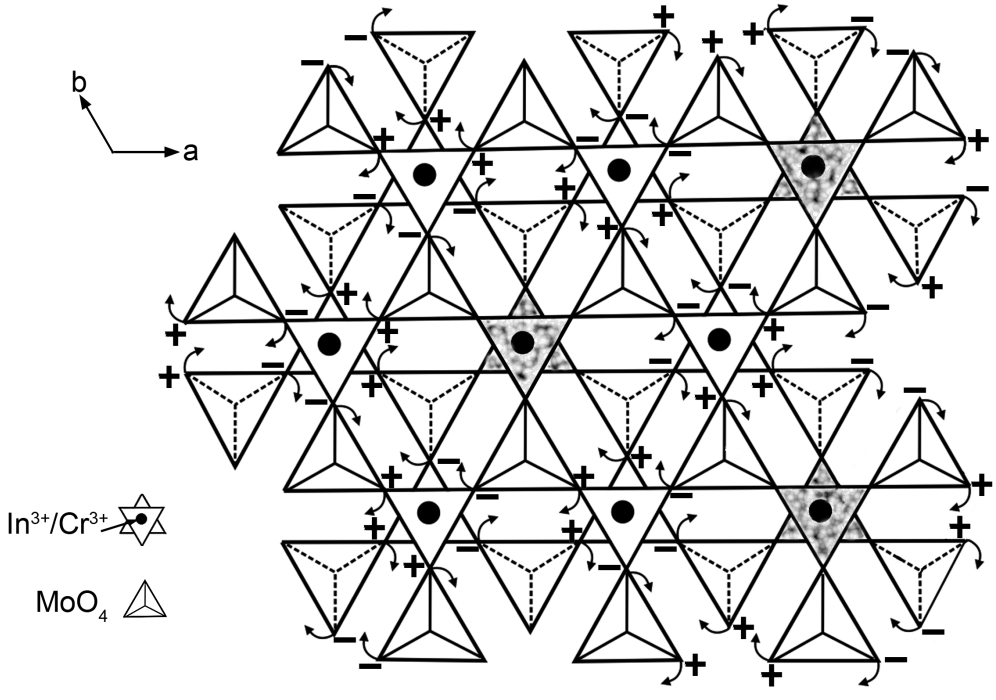

Figure 5: The scheme of possible distortion of the crystal structure in $RbIn(MoO_4)_2$ below T_5=84 K. Only one layer $\{[In(MoO_4)_2]^-\}_{\infty\infty}$ is shown.

This type of deformation can be considered as result of two different rotations of the MoO_4 groups: one around the twofold symmetry axis X, the other along the threefold symmetry axis Z. To retain the trigonal symmetry of the crystal in its lowest phase, a doubling of the lattice constant *c* is required. The deformation of the next layer of

crystal structure can be obtained by the operation of either the *c*-type mirror plane or the twofold axis on the layer shown in Figure 5. The above acting would lead to 3m or 32 crystal point groups, respectively. More complex distortion, not shown here, can restore -3m symmetry.This low-temperature phase of $RbIn(MoO_4)_2$ seems to be new, unknown in the family of TDM/T crystals. For Aizu species -3mF32(or 3m) a certain ferroic ordering like antiferroelasticity or ferrogyrotropy could be speculated [135] . So one can expect such ordering in this phase of $RbIn(MoO_4)_2$ [60] .

III.2 $KSc(MoO_4)_2$

$KSc(MoO_4)_2$ crystal is one of the best studied crystals from the TDM/T family, in which a sequence of three ferroelastic phase transitions was discovered (Table 1). Earlier papers reported on the occurrence of two ferroelastic phase transitions in $KSc(MoO_4)_2$ [29] ; one of second order at T_1 = 260 K and the other of first order at about 183 K (later marked as T_3), which were confirmed by the Raman[73] and EPR of Cr^{3+} ions studies[87] .

Two soft modes of A_g and B_g symmetries and a gradual splitting of E_g-type mode present in the para- phase are observed in Raman spectra below T_1 [73]. The observed splitting of the doubly degenerate modes indicates a loss of trigonal symmetry. On basis of this study the conclusion was drawn that the transition does not involve significant distortion of the MoO_4 tetrahedral units and the phase transition mechanism is associated with $(MoO_4)^{2-}$ anion rotations and displacements of K^+ cations.

With regards to the temperature variations of the zero-field splitting (ZFS) tensor of Cr^{3+} complexes [87] a structural distortion model of the high-temperature phase was proposed, based on the motion of the oxygen atoms of the anion $(MoO_4)^{2-}$ that constitute the environment of Sc^{3+}. At that moment it was postulated that below 260 K the distortion leads to a monoclinic phase of space group symmetry C2/m, and below 183 K to a monoclinic phase with the space group C2/c.

The additional first-order phase transition was revealed by means of EPR study at about 240 K (marked as T_2) [48]; it was confirmed by x-ray and optical measurements [84]. It was stated that the transition at T_2 leads the crystal to the ferroelastic phase of C2/m symmetry [105] .

The detailed examination of domain structure thermal evolution by means of a polarizing microscope, aimed at elucidation of crystallographical features of the three ferroelastic $KSc(MoO_4)_2$ phases and phase transitions between them, was done in paper [99]. It was found that phase transitions are accompanied by changes of predominant type of ferroelastic domain walls. In the first and third ferroelastic phases the existence of tilted domain walls W` is preferable and there is a tendency to formation of polysynthetic twins Tw(W`). On the contrary, the domain pattern in the second phase shows lamellar domains with walls W. It was stated that all the phases

exhibit 2/m point symmetry and that the distortion of the optical indicatrix in (0001) cross-section has opposite sign in the second phase relative to both the first and third phases. Thus, the location of optical indicatrix axes n_g and n_m relatively to the internal symmetry elements of domains is as follow*:* n_g || *m,* n_m || 2 in the first and third phases, and n_g || 2, n_m || m in the second one. Phase transitions at T_2 and T_3 are accompanied by thermal hysteresis and hyperphotoelastic effect [98] .

TEM studies of $KSc(MoO_4)_2$ have revealed the presence of characteristic domain patterns with a high density of domain walls [40]. The average size of microdomains in the second ferroelastic phase is about 500 nm (at 214 K), while near T_3 the domains are smaller than 50 nm, and their wall width does not exceed 5 nm.

The phase transitions between individual ferroelastic phases in $KSc(MoO_4)_2$ feature a poor morphic birefringence anomaly $(\Delta n)_Z = n_g - n_m$, and in addition the $\Delta n(T)$ graph seems to have an almost identical course in all the three ferroelastic phases, despite an abrupt change in the orientation of n_g and n_m axes of these three phases [100]. A small anomaly in the temperature dependence of the morphic birefringence $(\Delta n)_Z$ is observed close to T_2, while a considerably large jump of $(\Delta n)_Z$ ($\approx 0.12 \times 10^{-3}$) is visible at T_3 [96].

Transitions to monoclinic ferroelastic phases in TDM/T may be manifested in the EPR spectra through the splitting of the EPR line into a few well resolved components, depending on the deformation of the crystal structure and crystal division into ferroelastic domains. However, in $KSc(MoO_4)_2$ the transition at T_1 is observed through the anomalous broadening of EPR lines and the unusual shape of the EPR spectrum; each the high-temperature resonance line is distributed into a broad continuum limited by edge singularities [48], presenting a typical EPR lineshape of structurally modulated crystals. Anomalous behavior of the EPR line was attributed to the presence of an incommensurate phase below 260 K, in which each ferroelastic domain is modulated in a single direction (1q state) but the direction of modulation wave varies from one domain to another [105,107]. Incommensurate-like resonance lines are seen in the EPR spectrum also below T_2, thus the transition to the second ferroelastic phase can be interpreted as an incomplete lock-in one.

In heat capacity studies [86] a λ-shaped anomaly was seen at the normal – incommensurate transition temperature (T_1), while no anomaly was detected at the supposed lock - in transformation temperature (T_2); a lack of any thermal anomaly in the vicinity of T_2 was explained by a pinning of the modulation wave vector to defects in this crystal. Incommensurate systems are in general very sensitive to defects of various kind [136]. The incommensurate phase in $KSc(MoO_4)_2$ is connected with the simultaneous appearance of the ferroelastic domain structure. Being created spontaneously the domain structure is probably an origin of defects; domain walls can play the role of defects in such systems [86,90].

The value of the critical index β in $KSc(MoO_4)_2$, as found from EPR studies of Gd^{3+} ions, is 0.33 [93]. Such a value is close to the one that characterizes incommensurate phase transitions rather than the second order ferroelastic phase transitions, for which one would expect the critical index to be equal to 0.5. It is also close to the value of critical index β found in mixed $Rb_xK_{1-x}Sc(MoO_4)_2$ with the low concentration of Rb ions: β = 0.32 for $Rb_{0.03}K_{0.97}Sc(MoO_4)_2$ and β = 0.33 for $Rb_{0.1}K_{0.9}Sc(MoO_4)_2$ [117] . Lower than 0.5 value of critical index β in $KSc(MoO_4)_2$ was also obtained from temperature dependence of elastic constants c_{11} (0.395) [80] .

The elastic properties of $KSc(MoO_4)_2$ have been studied using the ultrasonic method [82] and Brillouin spectroscopy[75,80]. Very detailed information about acoustic anomalies occurring in all the three phase transitions is presented by Maczka [80]. It was found that the transition at T_1 results in a very large drop in velocity of the lowest frequency transverse mode propagating along the Y and X axes. The observed changes in the elastic constants are consistent with the results of the ultrasonic measurements [82]. Large anomalies for the elastic constants c_{44} and c_{66} below T_1, corresponding to the strains e_4 and $e_1 - e_2$, are in agreement with the predictions of phenomenological theory [29].The unusual strong damping of the lowest frequency transverse mode, corresponding mainly to the elastic constants c_{44}, is observed below T_2. According to the authors, it may result from the presence of the residual discommensurations persisting below T_2 and it may be the indirect evidence that the phase transition at T_1 occurs to an incommensurate phase.

Published data on the third phase transition in $KSc(MoO_4)_2$ were not compatible with each other showing either triclinic [75,137] or monoclinic symmetry [87,99] below T_3. A character of observed changes in the Brillouin spectra supports the conclusion drawn from the EPR and optical measurements that the transition at T_2 occurs between the two predicted monoclinic structures C2/m and C2/c. The third transition at T_3 results in weak anomalies of elastic constants; this phase may have the same structure as the phase in the range 240–260 K [80].

Finally, the sequence of phase transitions in $KSc(MoO_4)_2$ proceeds as follows: P-3m1– T_1 → C2/c – T_2 → C2/m –T_3 → C2/c.

On the basis of EPR studies of admixture Cr^{3+} ions, models for the deformation of the trigonal structure leading to the monoclinic systems C2/m and C2/c were proposed [87,96]. The EPR results indicate that in the second ferroelastic phase (phase C2/m) two kinds of structurally nonequivalent chromium complexes appear, that differ both in the values of their ZFS parameters and the location of principal directions of their ZFS tensor. The *z*-axes of chromium complexes deviate from the threefold axis but remain in the YZ plane. The crystal structure distortion in the phase C2/m is shown schematically in Figure 6.

As a starting point, fragment of the projection of the crystal structure onto one of the *m*-planes of the paraelastic phase (ZY plane) is presented in Figure 6a. Here, the threefold axis Z coincides with the *z*-axis of the coordination environment of the ion Cr^{3+} (Sc^{3+}). A fundamental distortion of the unit cell in the temperature range $T_2<T<T_3$ K is in accordance with that reported in [87] for the monoclinic phase of C2/m symmetry and is presented in Figure 6b. It relies on a rotation of the CrO_6 (ScO_6) groups, occupying the unit cell levels z = 0 and c/2, in the two opposite directions around the twofold axis X, which results in a structural differentiation of the chromium complexes into types I and II.

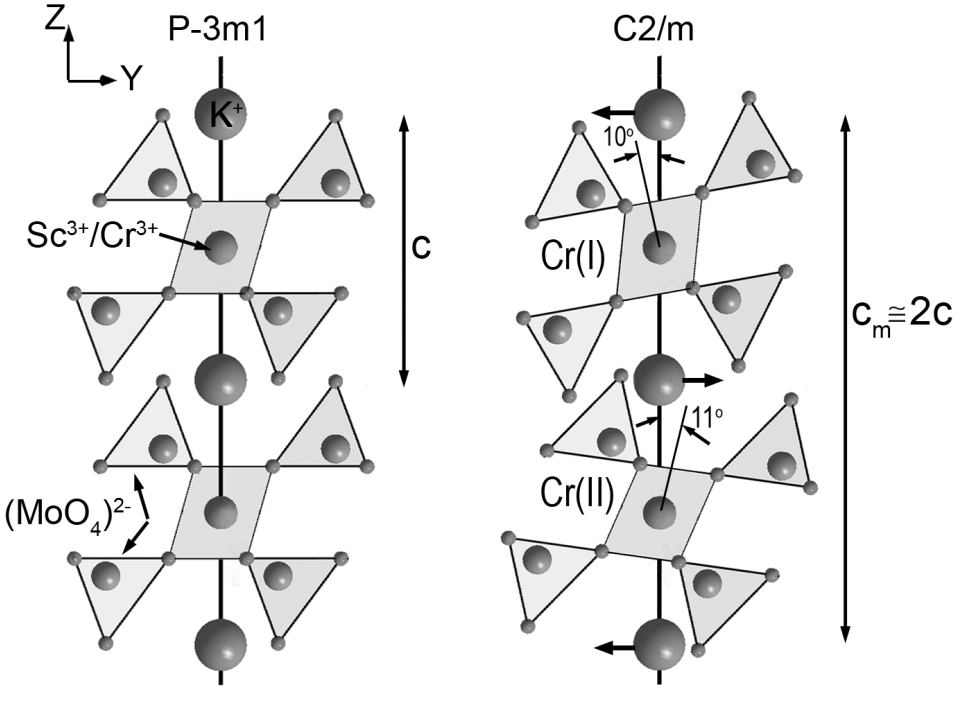

Figure 6: (a) Fragment of the projection of the $KSc(MoO_4)_2$ structure in the trigonal phase onto the *ZY* plane; (b) Projection of the same fragment onto the *ZY* plane, for the second ferroelastic phase. The deviation of the *z* axes from the initial direction is shown for Cr^{3+} complexes of types I and II.

This rotation is accompanied by an additional deformation of the coordination surroundings, as a result of which the crystal field loses its axial symmetry and two structurally non-equivalent paramagnetic centres differ also in values of the ZFS parameters.

The unit cell deformation proposed for the second ferroelastic phase must involve the unit cell contraction along the crystal Y-axis. In such a case the optical indicatrix axis n_g would be parallel to the X-axis, as observed experimentally. Thus, the model of deformation proposed above is consistent with the prediction for C2/m symmetry.

In the third ferroelastic phase all Cr^{3+} complexes are structurally equivalent and they have identical values of the ZFS parameters, but differ by the location of the principal axes of their ZFS tensor. The deformation of the unit cell in the third ferroelastic phase originates from an abrupt change of the oxygen ion positions and it can be regarded as a combination of two rotations around two different axes. Details of such rotations and a model of the crystal structure deformation for the third ferroelastic phase are given and discussed in papers [87] and [96]. This type of unit cell deformation results in structurally equivalent but magnetically non-equivalent chromium complexes and is consistent with a monoclinic C2/c symmetry. The model of deformation given in [97] allows to explain changes in the orientation of the optical indicatrix axes on transition from the second to third ferroelastic phase and a considerably great jump of $(\Delta n)_Z$ at the transition point between these phases.

Because of a substantial broadening of EPR lines, data concerning the ZFS tensor could not be obtained in the first ferroelastic phase. Therefore, an attempt to build a model of crystal structure deformation in the same way as for the other two ferroelastic phases was unsuccessful [96].

The results of x-ray structural studies of $KSc(MoO_4)_2$ at temperatures above T_1 could suggest another possible choice of the initial space group, i.e. P-3c1 (Z=2) [84]. This conclusion was based on the observation of non-zero intensity for reflections with odd l, which are forbidden for trigonal space group P-3m1. This choice of space group for $T > T_1$ seems to be questionable, because in this case two different types of paramagnetic centers should appear in the EPR spectrum, which is not observed experimentally.

III.3 $KFe(MoO_4)_2$

In $KFe(MoO_4)_2$ two ferroelastic phase transitions occur: a second-order transition at T_1 = 311 K [46] and the other of first order revealed at T_2 = 139 K [47]. The transition at T_1 is manifested by considerable changes in Raman spectra. The most interesting behaviour displays the low frequency part of the spectra (0-50 cm^{-1}) in which four new phonon modes ($2A_g+2B_g$) appear in the ferroelastic phase, of which two ($A_g(1)$ and

B(1)) behave as soft modes [47]. It was found that in the interval $0.45 \leq T/T_1 \leq 0.9$ the $A_g(1)$ soft mode frequency varies as $(T_1\text{-}T)^{0.35}$.

The confirmation of the second phase transition was obtained by specific heat and birefringence measurements [74]. A sharp narrow maximum was observed at T_2 in the specific heat whereas no anomaly is detected at T_1. The phase transition at T_2 is connected with a discontinuous decrease of birefringence $(\Delta n)_Z = n_g - n_m$. No rotation of the optical indicatrix and no reconstruction of domain structure at T_2 was observed, either. All mentioned above facts show that after the second transition $KFe(MoO_4)_2$ remains monoclinic [74]. Both ferroelastic phases seem to have the same space group; the monoclinic symmetry C2/m was suggested in [36] whereas the symmetry C2/c in [47].

Elastic constants of $KFe(MoO_4)_2$ were examined by Brillouin scattering. It was stated that a behaviour of elastic constants near the two phase transitions differs strongly. The compression elastic constants c_{11} and c_{22} show no anomaly whereas a large anomaly is observed for shear elastic constant at T_1. At T_2 considerable anomaly is observed for c_{22} [74].

More detailed microscopic studies [102] resulted in discovering that phase transition at T_2 (reported first in [74] as occurring at the temperature of 139 K) in fact takes place in two stages, as two transitions close to each other at $T_2 = 134.3$ K and $T_3 = 133.9$ K in heating run, with the temperature interval of 0.4 K between them. Both these transitions are of the first order and are evidenced through a phase front passing, without the domain structure rebuilding. From temperature studies of the morphic birefringence, a critical exponent value of the order parameter has been estimated as $\beta = 0.34$ [102]; this value is close to that found from the temperature dependence of soft-mode frequencies ($\beta = 0.35$) [74]. The value obtained is close to the critical exponent values that describe the behavior of order parameter in other crystals of the TDM/T family, e.g. $\beta = 0.33$ for $KSc(MoO_4)_2$ [93] and $\beta = 0.34$ for $KSc(WO_4)_2$ [94].

The disposition of optical indicatrix axes n_g and n_m has been established [102]. At room temperature the optical indicatrix axes feature the following orientation: the axis $n_g \parallel 2$, and the axis $n_m \parallel m$ and this location does not change when the $KFe(MoO_4)_2$ crystal passes the subsequent ferroelastic phases. Such a behavior is different from that observed in the $KSc(MoO_4)_2$ model crystal, where transitions to consecutive monoclinic ferroelastic phases each time cause a reciprocal change of the n_g and n_m axes orientation [99]. Taking into account this position of indicatrix axes it can be assumed that in all ferroelastic phases in $KFe(MoO_4)_2$, the monoclinic system with symmetry C2/m is executed. This symmetry is also in agreement with the results obtained from magnetic resonance studies [125]. The authors have found that below T_1 the triangular structure of $KFe(MoO_4)_2$ crystal is distorted and the crystal contains layers of magnetic ions Fe^{3+}(I) and Fe^{3+}(II) occurring in the non-equivalent positions of two types; only the group C2/m enables non-equivalent adjacent magnetic layers.

Recently, $KFe(MoO_4)_2$ attracted considerable attention since the compound constitutes an example of triangular lattice antiferromagnet [125]. Collinear and helical, commensurate and incommensurate structures, that are ordered in either three or two dimensions and reside simultaneously and independently on alternating intercalated magnetic layers, were reported below T_N = 2.5 K. Such peculiar magnetic ordering, not known in any other triangular lattice antiferromagnet materials, is due to lattice distortions occurring at the phase transitions at T_1 and T_2 [126].

IV. Conclusion

Studies of double molybdates and tungstates, started over 50 years ago in search of new laser crystals, have led to a discovery of trigonal double molybdates and tungstates, a group of crystals with specific ferroic properties. This review is devoted to this group of materials.

Our attention was paid on ferroelastic phase transitions occuring in most of them. In particular, the successive phase transitions occurring in the $RbIn(MoO_4)_2$, $KSc(MoO_4)_2$ and $KFe(MoO_4)_2$ crystals were discussed in detail. It is worth noting that ferroelastic phase transitions in $RbIn(MoO_4)_2$ and $KSc(MoO_4)_2$ could be combined with an incommensurate modulation of their structures. Furthermore, the phase present in $RbIn(MoO_4)_2$ below 84 K does not fit into the scheme of transitions predicted by phenomenological theory. Also pecularities of ferroelastic domain structures, accompanying transitions from the trigonal-to-monoclinic phases in TDM/T were reported.

It was shown that EPR spectroscopy with paramagnetic spin probes can be succesfully used for probing structural changes taking place in the TDM/T crystals. Based on the movement of oxygen atoms of anions $(MoO_4)^{2-}$ constituting the surrounding of trivalent cations, possible models of structural distortions on transition to monoclinic phases were discussed for $KSc(MoO_4)_2$ and $RbIn(MoO_4)_2$. It has been concluded that the local structure distortion in these crystals is more complex than that resulting from the phenomenological description of ferroelastic phase transitions in TDM/T.

Publications regarding the local symmetry changes during transitions to the ferroelastic phases in TDM/T are mainly based on the results of Raman, Brillouin and EPR studies. Unfortunately, there is a lack of papers devoted to determination of the structure in the succesive ferroelastic phases in TDM/T by diffraction methods.

Due to the fact that magnetic Fe^{3+} ions form a simple haxagonal network so called 120º structure, iron molybdates $AFe(MoO_4)_2$ (A = K,Cs,Rb), have turned out to be good models of two-dimensional triangular anti-ferromagnet. In particular, $RbFe(MoO_4)_2$ becomes a subject of intense investigations since the magnetically induced ferroelectricity driven by the in-plane spin chirality of the 120°structure have lately been revealed in it. TDM/T materials can also be considered as potential candidates for broadband laser applications.

Cite this paper: M.B.Zapart and W.Zapart, OAJ materials and Devices, vol 5(1) – chap No10 in "Perovskites and other Framework Structure Crystalline Materials", p327 (Coll. Acad. 2021) DOI:10.23647/ca.md20202708

REFERENCES

1. V.K.Trunov, V.A.Efremov, Y.A.Velihkodnyi, Crystallochemistry and Properties of Double Molybdates and Tungstates, Nauka, Leningrad,USSR(1986)
2. V.A.Isupov, *Ferroelectrics,* **vol.321,** p 63 (2005)
3. K.Nassau, H.J.Levinstein, G.M.Loiacono, *J.Phys.Chem.Solids* ,**vol.26,** p 1805 (1965)
4. E.Gallucci, C.Goutaudier, F.Bourgeois, G.Boulon, M.Th.Cohen-Adad, *J.Solid State Chem.,* **vol.163**, p 506 (2002)
5. P.V.Klevtsov, R.F.Klevtsova, *J. Struct.Chem*., **vol.18**, p 339 (1977)
6. V.A.Morozov, A.V.Arakcheeva, G.Chapuis, N.Gublin, M.D.Rossell, G.Van Tendeloo, *Chem. Mater.,* **vol.18**, p 4075 (2006)
7. A.V.Arakcheeva, P.Pattison, G.Chapuis, M.Rossell, A.Filaretov,V.Morozov, G.Van Tendeloo, *Acta Crystallogr.*B, **vol.64**, p 160 (2008)
8. V.A.Morozov, A.V.Arakcheeva, P.Pattison, K.W. Meert, P.F.Smet, D.Poelman, N.Gauquelin, J.Verbeeck, A.M.Abakumov, J. Hadermann, *Chem. Mater.*,**vol. 27**, p 5519 (2015)
9. W.Guo, Y.Lin, X.Gong, Y.Chen, Z.Luo, Y.Huang, *J. Phys. Chem. Solids*, **vol.69**, p 8 (2008)
10. Y.J.Chen, Y.F.Lin, X.H.Gong, Q.G.Tan, Z.D.Luo, Y.D.Huang, *J.Opt. Soc. Am*., **vol. 24 B**, p 496 (2007)
11. J.Liu, J.M.Cano-Torres, C.Cascales, F.Esteban-Betegón, M.D.Serrano, V.Volkov, C.Zaldo, M.Rico, U.Griebner, V.Petrov, *Phys. Status Solidi A*, **vol.202**, p R29 (2005)
12. A.A.Kaminskii, *Laser crystals and ceramics: recent advances*, *Laser & Photon. Rev*., **vol.1**, p 93 (2007)
13. B.Glorieux, V.Jubera, A.Apheceixborde, A.Garcia, *Solid State Sci.*, Elsevier, **vol. 13**, p 460 (2011)

14. Y.Liu , H.Zuo, J.Li, X.Shi , S.Ma, M.Zhao, K.Zhang, Ch.Wang, *Ceram. Int.*,**vol.42**, p 7781 (2016)
15. H.W.Yang, J.X.Zhao, H.T.Huang,J.L.He, *Laser Phys.,* **vol.21**, 343 (2011)
16. S.Ding, X.Zhang, Q.Wang, F.Su, P.Jia, S.Li, S.Fan, J.Chang, S.Zhang, Z.Liu*, IEEE J. Quantum Elect.*, **vol. 42**, p 927 (2006)
17. E.W.Barrera, Q.Madueńo, F.J.Novegil, A.Speghini, M.Bettinelli, *Opt.Mater.*, **vol.84**, p 354 (2018)
18. M.Pollnau, Y.E.Romanyuk, F.Gardillou, C.N.Borca, U.Griebner, S.Rivier, V.Petrov*, IEEE J. Selected Topics in Quantum Elect.*, **vol.13**, p 661 (2007)
19. E.F.Dudnik, T.M.Stolpakova, *Fiz.Tverd.Tela***, vol.17**, p 3405 (1975)
20. E.F.Dudnik, T.M.Stolpakova, *Ukr. Fiz. Zh.,* **vol.21,** p 1211 (1976)
21. A.Pena, R.Sole, Jna.Gavalda, J.Massons, F.Diaz, M.Aguilo, *Chem. Mater. ,* **vol.18***,* p 442 (2006**)**
22. R.F.Klevtsova, P.V.Klevtsov, *Kristallografiya*, **vol.15**, p 953 (1970)
23. R.F.Klevtsova, *Dokl. Akad. Nauk SSSR*, **vol. 221**(6), p. 1322 (1975)
24. K.Brandenburg, DIAMOND version 3.0e, Crystal Impact GbR, Bonn (2005)
25. P.V.Klevtsov, L.P.Kozeeva, L.Yu.Kharchenko, *Kristallografiya,* **vol.20**, p 1210 (1975)
26. G.Wang, X.Han, M.Song , Z.Lin, G.Wang, X.Long, *Mater.Lett.,* **vol.61,** p 3886 (2007)
27. M.Maczka, K.Hermanowicz, P.E.Tomaszewski, M.Zawadzki, J.Hanuza, *Opt.Mater.,* **vol.31**, p 167 (2008)
28. I.Koseva, V.Nikolov, A.Yordanova, P.Tzvetkov, D.Kovacheva, *J.Alloy Compd.*, **vol.509**, p 7022 (2011)
29. A.I.Otko, N.M.Nesterenko, L.V.Povstyanyi, *Phys. Status Solidi A,* **vol.46**, p 577 (1978)
30. N.M.Nesterenko, V.I.Fomin, V.I.Kutьko, *Fiz.Nizk.Temp.,* **vol.8**, p 862 (1982)
31. E.F.Dudnik, E.V.Siniakov, T.M.Stolpakova, G.V.Dovchenko, *Fiz.Tverd.Tela,* **vol.5**, p 1401 (1976)
32. A.I.Otko, N.M.Nesterenko, *Ukr. Fiz. Zh.,* **vol 24**, p 1048 (1979)
33. E.V.Sinyakov , E.F.Dudnik, T.M.Stolpakova, O.L.Orlov, *Ferroelectrics,* **vol.21**, p 579 (1978)
34. A.I.Otko , N.M.Nesterenko, G.G.Krainyuk, A.E.Nosenko, *Ferroelectrics,* **vol.48,** p 143 (1983)
35. E.F.Dudnik, G.A.Kiosse, T.M.Stolpakowa*, Izv. AN. SSSR Fiz.,* **vol.47**(3), p 504 (1983)
36. E.F.Dudnik ,T.M. Stolpakowa, G.A.Kiosse*, Izv. AN. SSSR Fiz.,* **vol. 50**, p 2249 (1986)
37. G.G.Krainyuk, A.E.Nosenko, A.I.Otko, *Ferroelectrics,* **vol.48**, p 175 (1983)
38. G.G.Krajniuk, A.I.Otko, A.E.Nosenko, *Izv. AN. SSSR Fiz.,* **vol. 47** (4), p 758 (1983)
39. A.I.Otko, G.G.Krainyuk, T.M.Stolpakova, E.F.Dudnik, *Izv.AN. SSSR Fiz.,* **vol.48**(6), p 1116 (1984)
40. M.B.Zapart, E.Snoeck, P.Saint-Gregoire*, Ferroelectrics*, **vol. 191**, p 179(1997)
41. R.Kowalczyk, M.B.Zapart, W.Zapart, *Ferroelectrics,* **vol. 441**, p 33 (2012)
42. M.B.Zapart, W.Zapart, R.Kowalczyk, *Ferroic Materials by Polarized Ligth Microscopy and AFM* in monograph: *Physics 2013 - Physical basis of properties of selected crystalline, amorphous and molecular materials*. Ed. K.Dziliński, J.J.Wysłocki, Technical University, Czestochowa 2013 (in Polish) ISBN 978-83-63989-07-1 ISSN 2080-2072
43. M.Maczka, K.Hermanowicz, P.E.Tomaszewski, J.Hanuza, *J.Phys.-Condens. Matter*,

vol.16, p 3319 (2004)

44. K.Hermanowicz, M.Maczka, P.J.Deren, J.Hanuza, W.Strek, H.Drulis, *J. Lumin.,* **vol. 92**, p 151 (2001)
45. P.V.Trunov, V.A.Efremov, *Zh. Neorg. Khim*. **vol.16**, p 2026 (1971)
46. A.I.Otko, L.N.Pelikh, L.V.Povstyanyi, N.M.Nesterenko, P.S.Kalinin, A.I.Zvyagin, *Izv.AN.SSSR Fiz.,* **vol.39**, p 697 (1975)
47. G.A.Smolenskii, I.G.Sinij, E.F.Kuzminov, E.F.Dudnik, *Izv. AN. SSSR Fiz.,* **vol.43**, p 1650 (1979)
48. W.Zapart, M.B.Zapart, *Phys.Status Solidi A*, **vol. 121**, p K43 (1990)
49. V.A.Balashov, M.P.Slisskaya, L.S.Zevin, Z.K.Zolina, A.A.Maier, *Kristallografiya,* **vol.17**, p 1245 (1972)
50. W.Zapart, M.B.Zapart, A.I.Otko, *Ferroelectrics,* **vol. 107**, p 343 (1990)
51. M.B.Zapart,W.Zapart, *Ferroelectrics*, **vol.192,** p 81 (1997)
52. P.V.Klevtsov, L.P.Kozeeva, L.Yu.Kharchenko, *Kristallografiya,* **vol.20**, p 1210 (1975)
53. W.Zapart, M.B.Zapart, *Ferroelectrics*, vo**l. 497,** p 126 (2016)
54. V.Klevtsov, R.F.Klevtsova, A.V.Demenev, *Kristallografiya,* **vol.17**, p 545 (1972)
55. V.A.Efremov V.K.Trunov, Yu.A.Velikodnyi, *Kristallografiya,* **vol.16**, p 1052 (1971)
56. M.B.Zapart, J.Stankowski., B.Sczaniecki, A.I.Otko, *Acta Phys. Pol.A,* **vol.66,** p 445 (1979)
57. W.Zapart, M.B.Zapart, *Phase Transit.,* **vol.84**, p 872 (2011)
58. M.B.Zapart, W.Zapart, A.I.Zvyagin, *Phys.Status Solidi A,* **vol. 82**, p 67 (1984)
59. W.Zapart, *Ferroelectrics,* **vol. 105**, p.291 (1990)
60. W.Zapart, M.B.Zapart, W.Schranz, M.Reinecker, *Phase Transit.,* **vol. 86**, p 123 (2013)
51. M.B.Zapart,W.Zapart, *Ferroelectrics*, **vol.192,** p 81 (1997)
52. P.V.Klevtsov, L.P.Kozeeva, L.Yu.Kharchenko, *Kristallografiya,* **vol.20**, p 1210 (1975)
53. W.Zapart, M.B.Zapart, *Ferroelectrics*, vo**l. 497,** p 126 (2016)
54. V.Klevtsov, R.F.Klevtsova, A.V.Demenev, *Kristallografiya,* **vol.17**, p 545 (1972)
55. V.A.Efremov V.K.Trunov, Yu.A.Velikodnyi, *Kristallografiya,* **vol.16**, p 1052 (1971)
56. M.B.Zapart, J.Stankowski., B.Sczaniecki, A.I.Otko, *Acta Phys. Pol.A,* **vol.66**, p 445 (1979)
57. W.Zapart, M.B.Zapart, *Phase Transit.,* **vol.84**, p 872 (2011)
58. M.B.Zapart, W.Zapart, A.I.Zvyagin, *Phys.Status Solidi A,* **vol. 82**, p 67 (1984)
59. W.Zapart, *Ferroelectrics,* **vol. 105**, p.291 (1990)
60. W.Zapart, M.B.Zapart, W.Schranz, M.Reinecker, *Phase Transit.,* **vol. 86**, p 123 (2013)
61. S.A.Klimin, M.N.Popova, B.N.Mavrin, P.H.M. van Loosdrecht, L.E.Svistov, A.I.Smirnov, L.A.Prozorova, H.A.Krug von Nidda, Z.Seidov, A.Loidl, A.Ya.Shapiro, L.N.Demianets, *Phys. Rev. B*, **vol**.**68**, p 174408 (2003)
62. K.Hermanowicz, *J.Lumin.*, **vol.109**, p 9 (2004)
63. A.Gagor, P.Zajdel, D.Tobbens, *J. Alloy Compd.,* **vol.607**, p 104 (2014)
64. P.E.Tomaszewski, A.Pietraszko, M.Maczka, J.Hanuza, *Acta Crystallogr.,* **vol.75**, p 483 (1987)
65. A.A.Gurskas, V.B.Kokshenev, E.S.Syrkin, *Ferroelectrics*, **vol.75**, p 483 (1987)
66. U.Kolitsch ,M.Maczka, J.Hanuza, *Acta Crystallogr. E,* **vol. 59**, p i10 (2003)

67. M.Maczka, S.Kojima ,J.Hanuza*, J. Raman Spectrosc*., **vol.30**, p 339 (1999)
68. I.Nikolov, V.Nikolov, P.Peshev, *J.Cryst. Growth,* **vol. 254**, p 107 (2003)
69. M.Maczka, K.Hermanowicz, L.Kepinski, J.Hanuza, A.Yordanova, I.Koseva, *Opt. Mater.,* **vol. 35** ,p 338 (2013)
70. M.Maczka, J.Hanuza, S.Kojima, J.H.van der Maas, *J.Solid State Chem.,* **vol.158**, p 334 (2001).
71. L.N.Pelikh, *Fiz.Tverd.Tela***, vol.24**(10), p 3145 (1982)
72. E.S.Syrkin,S.B.Feodosev,L.N.Pelikh,A.A.Gurskas, *Fiz.Tverd.Tela***, vol.24**(7), p 2076 (1982)
73. N.M.Nesterenko, V.I.Fomin, *Phys.Status Solidi A,* **vol. 51,** p K101 (1979)
74. G.A.Smolensky**,** S.D.Prokhorova, G**.**Siny, *Ferroelectrics,* **vol. 26**, p 677 (1980)
75. N.M.Nesterenko, V.I.Fomin, Yu.A**.**Popkov, A.I.Otko, *Fiz.Nizk.Temp.,* **vol.8**, p 87 (1982)
76. M.Maczka, J.Hanuza, E.T.G.Lutz, J.H.van der Maas, *J.Solid State Chem.* **vol**.**145**, p 751 (1999)
77. M.Maczka, S.Kojima,J.Hanuza*, J.Phys.Soc.Jpn*., **vol.68**, p 1948 (1999)
78. M.Maczka, S.Kojima,J.Hanuza, *Ferroelectrics*, **vol.229**, p 165 (1999)
79. M.Maczka, K.Hermanowicz, P.E.Tomaszewski, J.Hanuza, *J. Phys.-Condens. Matter,* **vol.16**, p 3319 (2004)
80. M.Maczka, J.Hanuza, F.Jiang, S.Kojima, *Phys. Rev. B*, **vol. 63**, p 144101 (2001)
81. M.Maczka, F.Jiang, S.Kojima, J.Hanuza, *J.Mol. Struct.*, **vol.563-564**, p 365 (2001)
82. G.A.Zvyagina, V.D.Fil, I.G.Kolobov, S.V.Zherlitsyn, *Ferroelectrics* ,**vol.130**, p 315 (1992)
83. W.Zapart , *Phys. Status Solidi A,* **vol.118**, p 447 (1990)
84. I.A.Kislov, V.V.Mitkeich, N.M.Nesterenko, S.M.Tret'yak, *Kristallografiya,* **vol.36**, p 1298 (1991)
85. N.M.Nesterenko, V.I.Fomin, A.V.Peschanskii, V.V.Mitkevich, *Ferroelectrics*, **vol.239**, p 101 (2000)
86. M.Maczka, S.Kojima, J.Hanuza, *J. Phys. Chem. Solids,* **vol.59**, p 1429 (1998)
87. M.B.Zapart, W.Zapart, J.Stankowski, A.I.Zviagin, *Physica B,* **vol.114**, p 201 (1982)
88. W.Zapart, *Ferroelectrics*, **vol. 97**, p 137 (1989)
89. W.Zapart, M.B.Zapart, *Physica B,* **vol. 132**, p 359 (1985)
90. M.B.Zapart, *Ferroelectrics,* **vol. 137,** p 191 (1992)
91. M.B.Zapart, *Ferroelectrics,* **vol. 125,** p 355 (1992)
92. M.B.Zapart**,** *Ferroelectrics,* **vol. 172,** p 337 (1995)
93. M.B.Zapart, W.Zapart, P.Reng, A.I.Otko, *Ferroelectrics,* **vol. 272**, p 187 (2002)
94. W.Zapart, M.B.Zapart, P.Reng, J.Hanuza, M.Maczka, *Ferroelectrics*, **vol.337**, p 117 (2006)
95. W.Zapart, M.B.Zapart, *Ferroelectrics,* **vol. 451**, p 116 (2013)
96. W.Zapart, M.B.Zapart, *Phase Transit.,* **vol. 87**, p 1086 (2014)
97. K.Hermanowicz, *J.Alloy Compd.,* **vol. 341**, p 179 (2002)
98. A.I.Otko, W.Zapart, M.B.Zapart, V.B.Kapustianik, O.Kusznir, *Ferroelectrics***, vol. 141**, p 43 (1993)
99. A.I.Otko, M.Polomska, M.B.Zapart, W.Zapart, *Ferroelectrics***, vol. 172**, p 299 (1995)

100. A. I.Otko, J.Dec, S.Miga, *Ferroelectrics***, vol. 191**, p 253 (1997)
101. M.B.Zapart, W.Zapart, *Ukr.J.Phys.Opt.*, **vol.13**, p 196 (2012)
102. W.Zapart, M.B.Zapart, *Ferroelectrics*, **vol. 89**, p 761 (2016)
103. M.B.Zapart, W.Zapart, M.Maczka, *Ferroelectrics,* **vol. 497,** p 34 (2016)
104. W.Zapart, *Solid State Commun*., **vol. 76**, p 959 (1990)
105. W.Zapart, *Phase Transit.,* **vol. 34**, p 161 (1991)
106. M.B.Zapart, W.Zapart, *Ferroelectrics*, **vol. 137**, p 199 (1992)
107. M.B.Zapart, *Ferroelectrics,* **vol. 141**, p 67 (1993)
108. M.B.Zapart, W.Zapart, *Phase Transit.*, **vol. 43**, p 173 (1993)
109. M.B.Zapart, *Phase Transit.*, **vol. 43**, p 179 (1993)
110. P.Saint-Gregoire, *Ferroelectrics,* **vol. 175**, p 25 (1996)
111. N.M.Nesterenko, V.I.Fomin, Yu.A. Popkov, A.A.Gurskas, *Phys Status Solidi A,* **vol. 62**, p K35 (1980)
112. L.N.Pelikh, A.A.Gurskas, *Fiz.Tverd. Tela,* **vol. 23**, p 2169 (1981)
113. E.S.Syrkin, S.B.Feodosiev, L.N.Pelikh, A.A.Gurskas, *Fiz.Tverd Tela.* **vol**. **24**, p 2076 (1982)
114. L.N.Pelikh, *Ukr. Fiz. Zh.,* **vol. 28**, p 939 (1983)
115. W.Zapart, M.B.Zapart, K.Maternicki, R.Kowalczyk, M.Maczka, A.Winiarski, *Phase Transit.*,**vol. 83**, p 884 (2010)
116. W.Zapart, M.B.Zapart, N. M. Nesterenko, *Ferroelectrics,* **vol. 462**, p 110 (2014)
117. W.Zapart, M.B.Zapart, R.Kowalczyk, K.Maternicki, M.Maczka, *Ferroelectrics,* **vol. 418**, p 164 (2011)
118. M.B.Zapart, W.Zapart, A.I.Zvyagin, *Ferroelectrics,* **vol. 80**, p 63 (1988)
119. G.D.Saraiva, M.Maczka, P.T.C.Freire, J.Mendes Filho, F.E.Melo, J.Hanuza, Y.Morioka, A.G.Souza Filho, *Phys Rev B*., **vol. 67**, p 224108 (2003)
120. W.Paraguassu, A.G.Souza Filho, M.Maczka, P.T.C.Freire, F.E.Melo, J.Mendes Filho, J.Hanuza, *J.Phys.-Condens Matter* , **vol. 16**, p 5151 (2004)
121. M.Maczka A.Pietraszko, G.D.Saraiva, A.G.Souza Filho, W.Paraguassu, V.Lemos, C.A.Perottoni, **,** M.R.Gallas, P.T.C.Freire,P.E.Tomaszewski, F.E.Melo, J.Mendes Filho, J.Hanuza, *J.Phys.-Condens Matter.* **vol. 17**, p 6285 (2005)
122. A.Waskowska, L.Gerward, J.Staun Olsen, W.Morgenroth, M.Maczka, K.Hermanowicz, *J.Phys.-Condens. Matter* **vol. 22**, p 055406 (2010)
123. M.Maczka, M.Ptak, C.Luz-Lima, P.TC.Freire, W.Paraguassu, S.Guerini, J.Hanuza , *J Solid State Chem.,* **vol. 184**, p 2812 (2011)
124. M.Maczka, A.G.Souza Filho, W.Paraguassu, P.T.C.Freire, J.Mendes Filho, J.Hanuza, *Prog.Mater.Sci.,* **vol. 57**, p 1335 (2012)
125. L.E.Svistov, A.I.Smirnov, L.A.Prozorova, O.A.Petrenko, A.Ya.Shapiro, L.N.Dem'yanets, *JETP Lett.,* **vol. 80**, p 204 (2004)12
126. A.I.Smirnov, L.E.Svistov, L.A.Prozorova, A.Zheludev, M.D.Lumsden, E.Ressouche, O.A.Petrenko, K.Nishikawa, S.Kimura, M.Hagiwara,K.Kindo, A.Ya.Shapiro, L.N.Demianets, *Phys.Rev.Lett.,* **vol. 102**, p 037202 (2009)
127. T.Inami, *J.Solid State Chem.,* **vol. 180**, p 2075 (2007)

128. M.Kenzelmann, G.Lawes, A.B.Harris, G.Gasparovic, C.Broholm, A.P.Ramirez, G.A.Jorge, M.Jaime, S.Park, Q. Huang, A.Ya.Shapiro, L.A.Demianets, Phys. Rev. Lett., **vol. 98**, p 267205 (2007)

129. J.S.White, Ch.Niedermayer, G.Gasparovic, C.Broholm, J.M.S.Park, A.Ya.Shapiro, L.A.Demianets, M.Kenzelmann, *Phys.Rev. B,* **vol. 88**, p 060409(R) (2013)

130. G.Wang, Y.Huang, L.Zhang, Z.Lin, G.Wang, *Opt.Mater.,* **vol. 34**, p 1120 (2012)

131. K.Aizu, *J.Phys.Soc.Jpn.,* **vol. 28**, p 706 (1970)

132. J.Sapriel, *Phys. Rev. B,* **vol**.**12**, p 5128 (1975)

133. L.A.Shuvalov, N.R.Ivanov, O.A.Chikhadze, A.I.Izraelenko, *Kristallografiya*, **vol.18**, p 1207 (1973)

134. G.Wang, X.Long, L.Zhang, G.Wang, *J.Cryst. Growth,* **vol. 310**, p 624 (2008)

135. W.K.Wadhawan, *Classification of ferroic materials* in *Introduction to Ferroic Materials*, Gordon & Breach, Amsterdam, 2000.

136. P.Prelovšek, *Phase Transit.*, **vol. 11**, p 203 (1988)

137. V.I.Fomin, N.M.Nesterenko, *Kristallografiya,* **vol. 31**, p 818 (1986)